

THE MODELLISATION OF CONSTRAINED DAMPING LAYER TREATMENTS USING THE FINITE ELEMENT METHOD: SPATIAL MODEL AND VISCOELASTIC BEHAVIOUR

Rui Moreira ¹ José Dias Rodrigues ²

¹ Departamento de Engenharia Mecânica

Universidade de Aveiro, Campus Santiago, 3810-193 Aveiro – Portugal

² Faculdade de Engenharia da Universidade do Porto - DEMEGI

R. Dr. Roberto Frias, 4200-465 Porto – Portugal

SUMMARY: Surface and integrated damping treatments with viscoelastic layers play an important position among the passive damping treatments for light and flexible structures under vibration. Application simplicity, low cost, reduced structural modification and reduced additional mass, along with an inherent high efficiency, are the main reasons of its successful usage.

However, the design process of these treatments is not simple and requires a reliable tool for adequate designing and analysis.

The finite element method can be used for this purpose. However some considerations and special care are necessary to the spatial modelisation of the treatment and with the viscoelastic material properties characterisation.

In this work, a finite element commercial software (MSC/Nastran) was used to simulate the constrained and the integrated viscoelastic treatments applied on aluminium plates.

The spatial modeling of the treatment is developed using a layered scheme of plate/brick conventional finite elements. The dynamic properties of the viscoelastic material are taken into account in the numerical simulation using the complex modulus approach.

The numerical results are correlated with experimental data obtained in four treated specimens by direct comparison of the frequency response functions and by using some FRF-based correlation indicators.

KEYWORDS: Damping Layer Treatments, Viscoelastic Complex Modulus, FRF-Based Correlation

INTRODUCTION

The application of viscoelastic layers on light structures can provide a simple and reliable passive damping mechanism, particularly efficient under specific conditions of vibration [1,2,3].

The introduced damping is capable to control and reduce dynamic effects, such as high vibration levels and noise emission, and to extend working life of parts under cyclic loading or impact.

The damping treatments with viscoelastic layers can be applied on the surface of the vibrating structure, with or without a constraining layer, or integrated in the structure constituting a sandwich material, Fig.1, 2 and 3.

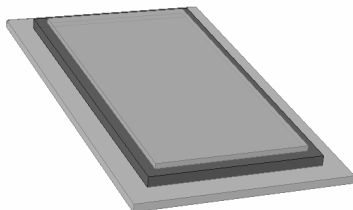


Fig.1: Surface treatment

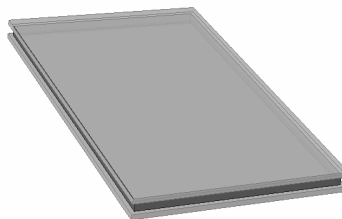


Fig.2: Integrated treatment

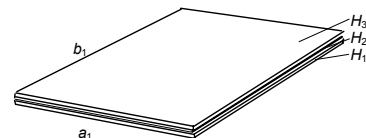


Fig.3: Damping treatment configuration

In the integrated (ILD) and constrained (CLD) layer damping treatments, the viscoelastic layer is strongly deformed in shear due to the effect of the constraining layer present in the constrained configuration or due to the adjacent skins of the integrated configuration.

This constraining effect is responsible by the large dissipation of the vibration energy that occurs within these treatments, thus being possible to have very effective treatments even with very thin damping layers that minimise the additional mass and the structural modification.

The surface treatments can be applied locally in specific and interesting areas of the structure, minimising the cost and the mass of the treatment, maintaining however the treatment effectiveness for some mode shapes or frequency range [3,4].

These treatments are widely used in the aeronautical and aerospace industry, where are the prime solution of passive damping treatments of light and large structures.

1. FINITE ELEMENT MODELISATION

The damping effect of the viscoelastic treatments can and should be predicted, and the treatments tailored, even during the design stage of the target structure.

The finite element method can provide a reliable tool in the design process of structures that incorporate this kind of treatments. However, there are two main aspects that should be considered during the application of this numerical tool. One is related to the spatial modelling of the viscoelastic layer, in order to get a realistic description of the high shear deformation pattern developed in this layer during the structure vibration motion. The other is related to the temperature and frequency dependence of the viscoelastic material properties and to the high loss factor that usually is exhibited by these materials.

1.1. SPATIAL MODEL OF THE TREATMENT

The damping mechanism of these treatments is closely related to the high shear deformation that occurs in the viscoelastic layer as a result of the restraint effect of the adjacent layers. Thus, it is very important to describe correctly the deformation of the dissipative layer. The Classical Laminate Plate Theory is not adequate to accurately describe the shear deformation of the viscoelastic layer, thus being necessary to use a different model [5,6].

All the three used models in this numerical study share a common representation of the viscoelastic layer using solid brick elements (HEXA8). The base plate and the constraining layer of the surface treatments, or the skin plates of the integrated layer configuration, are both modelled by either plate elements (QUAD4) or brick elements (HEXA8). The three used models in the numerical study are represented in Fig.4.

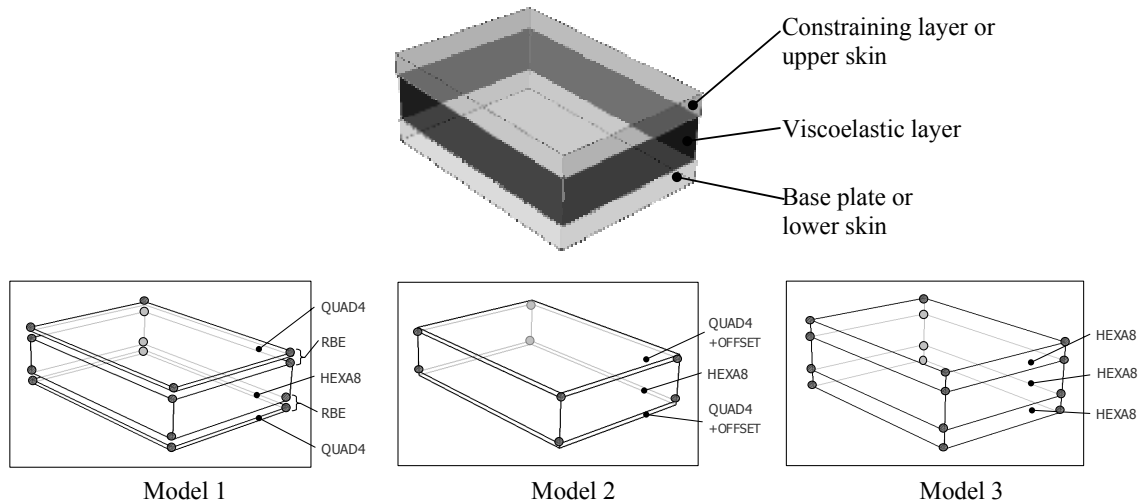


Fig.4: FEM models of the viscoelastic treatments

The first and second FEM models are quite similar. In the first, the plate's degrees of freedom are connected with the brick ones by means of rigid links (RBE) [7]. Using this model, the most complex one, it is possible to simulate bonding failures between the viscoelastic layer and the adjacent plates simply by removing those links in specific nodes of the FEM mesh.

In the second model, the plate element nodes are offset, by half of the plate thickness, to the plane in contact with the solid element, instead of the standard mid-plane. This results in coincident nodes and translational degrees of freedom between the plate and the adjacent face of the solid element. The last model uses solid elements to describe all the layers.

The three models considered have exactly the same total number of degrees of freedom. As they include solid brick elements, the spatial discretization must be refined enough to avoid shear-locking problems related to high area/thickness ratio.

The numerical results obtained are identical, independently of the model used. Nevertheless, model generation effort and time consuming are less important using model 2.

1.2. VISCOELASTIC MATERIAL MODELLING

The viscoelastic materials are characterised by a complex shear or extensional modulus exhibiting a large loss factor which is responsible for the dissipation effect, specially within the transition temperature range. Many authors [8,9,10] have been studying the modelling of the viscoelastic material characterization. Some of these have developed, based on the rheological models, formulations in time and frequency domains that require extra degrees of freedom to describe the material modulus behaviour with frequency.

Considering single harmonic excitation it is possible to use the complex modulus approach to describe the material behaviour in the frequency domain.

$$E(\omega, T) = E'(\omega, T) \cdot (1 + j\eta(\omega, T)) \quad (1)$$

Thus, the viscoelastic material is considered as an elastic material with a complex modulus of elasticity, where $E'(\omega, T)$ represents the storage modulus and $\eta(\omega, T)$ is the loss modulus of the viscoelastic material.

The complex modulus is usually represented as a function of temperature and frequency by the Reduced Frequency Nomogram [3]. The nomogram of the material 3M ISD112 [11] used in this study is represented in Fig.5.

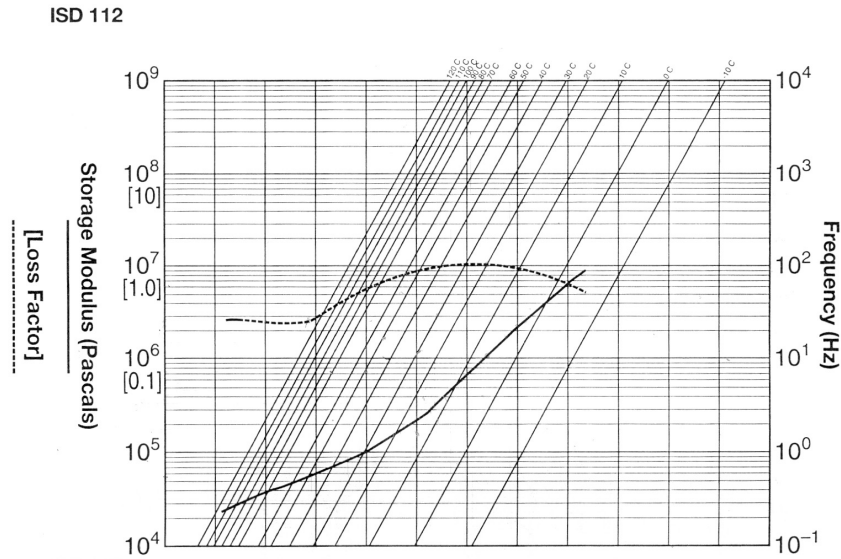


Fig.5.:Reduced-frequency nomogram of 3M ISD 112 [11]

1.3. FINITE ELEMENT SPATIAL MODEL

The finite element spatial model, defining the equations of motion of the system in matrix form, can be written as:

$$[M]\{\ddot{x}(t)\} + [K(\omega, T)]\{x(t)\} = \{f(t)\} \quad (2)$$

where $[M]$ is the mass matrix, $[K(\omega, T)]$ is the total stiffness matrix and $\{x(t)\}$ and $\{f(t)\}$ are, respectively, the forced response and the excitation vectors.

The stiffness matrix $[K(\omega, T)]$ contains the stiffness matrix of the base plate and of the constraining layer, which is a real entity, plus a complex stiffness matrix due to the viscoelastic layer:

$$[K(\omega, T)] = [K_e] + [K_v(\omega, T)] \quad (3)$$

The viscoelastic stiffness matrix is, therefore, a complex matrix whose terms depend on the temperature and frequency.

Considering an harmonic excitation of frequency ω as:

$$\{f(t)\} = \{F\} e^{j\omega t} \quad (4)$$

then, the steady state response of the system can be written as:

$$\{x(t)\} = \{\bar{X}\} e^{j\omega t} \quad (5)$$

where $\{\bar{X}\}$ is a complex vector. Substitution of Eqn 4 and Eqn 5 and its appropriate derivatives into Eqn 2 yields the algebraic set of equations:

$$[[K(\omega, T)] - \omega^2 [M]] \{\bar{X}\} = \{F\} \quad (6)$$

from which the vector $\{\bar{X}\}$, which depends on ω and the system parameters, can be obtained.

1.4. RESPONSE MODEL

The receptance frequency response functions for a reference k (input degree of freedom) are defined as:

$$\alpha_{jk}(\omega) = \left(\frac{\bar{X}_j(\omega)}{F_k} \right)_{F_i=0, \begin{cases} i=1, \dots, n \\ i \neq k \end{cases}} \quad (7)$$

These functions can be generated directly from the spatial model solving the Eqn 6 for different values of the excitation frequency ω :

$$[[K(\omega, T)] - \omega^2 [M]] \{\bar{X}(\omega)\}_k = \{F\}_k \quad (8)$$

where all the terms of the excitation vector of the system $\{F\}_k$ are equal to zero, except the one corresponding to the excitation degree of freedom.

If the temperature variable is considered as a constant entity, then the response model can be generated by a frequency sweep in which the complex stiffness matrix of the viscoelastic layer is recalculated at each frequency value, as represented in Fig.6.

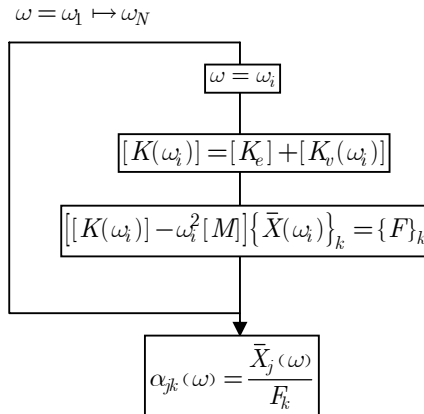


Fig.6: Response model generation diagram

2. EXPERIMENTAL STUDY

To validate the numerical models some frequency response functions were measured on four aluminium plates with CLD and ILD treatments. Table 1 presents the characteristics of the specimens used in this experimental study.

Table 1- Specimens used in the experimental study

Specimen	Dimensions a x b [mm]	H ₁ [mm]	H ₂ [mm]	H ₃ [mm]
1	298x197	2.0	0.125	0.250
2	297x197	2.0	0.125	0.200
3	298x198	1.0	0.250	1.0
4	298x198	1.0	0.125	1.0

The experimental specimens were supported by rubber bands to simulate free boundary conditions. A measuring mesh of 25 points was defined on each specimen, as represented in Fig. 7.

The plate was excited at point number 17 (the reference degree of freedom of this study) by a shaker driven by a random signal in the frequency band of [0,400 Hz]. The response velocity at each one of the mesh points was measured by a non-contact laser doppler measuring device (vibrometer). The experimental set-up is represented in Fig. 8.

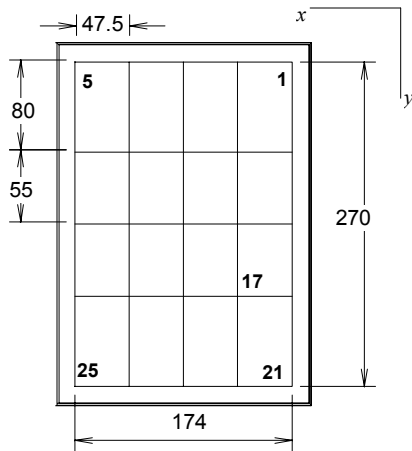


Fig. 7: Measuring mesh

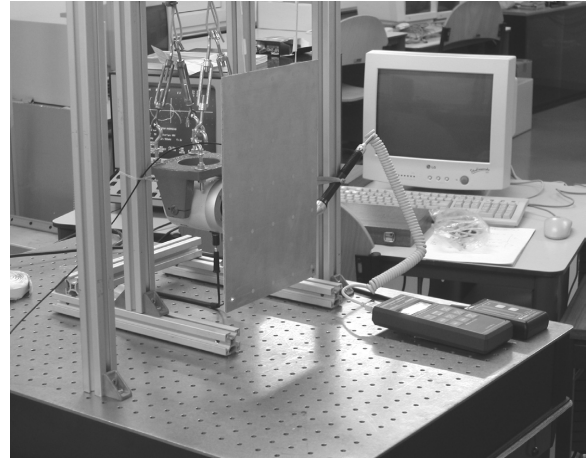


Fig.8: Experimental set-up

A dynamic signal analyser was used to acquire the excitation and the response signals. The velocity response signal was differentiated and the acceleration frequency response functions evaluated at each measuring point. Since the viscoelastic material properties are temperature dependent, the measurements were carried on near isothermal conditions, with temperature acquisition using a temperature probe.

3. EXPERIMENTAL RESULTS AND CORRELATION

3.1. TEMPERATURE EFFECTS

All the specimens were tested under isothermal conditions with a room temperature close to 17.5°C. Specimens 1 and 3 were also tested at a lower temperature (11.5°C).

The direct acceleration frequency response functions measured in specimen 3 at temperatures of 11.5°C and 17.5°C are represented in Fig.9. The graphic shows that it is very important, concerning the design process, to know the temperature conditions of the application.

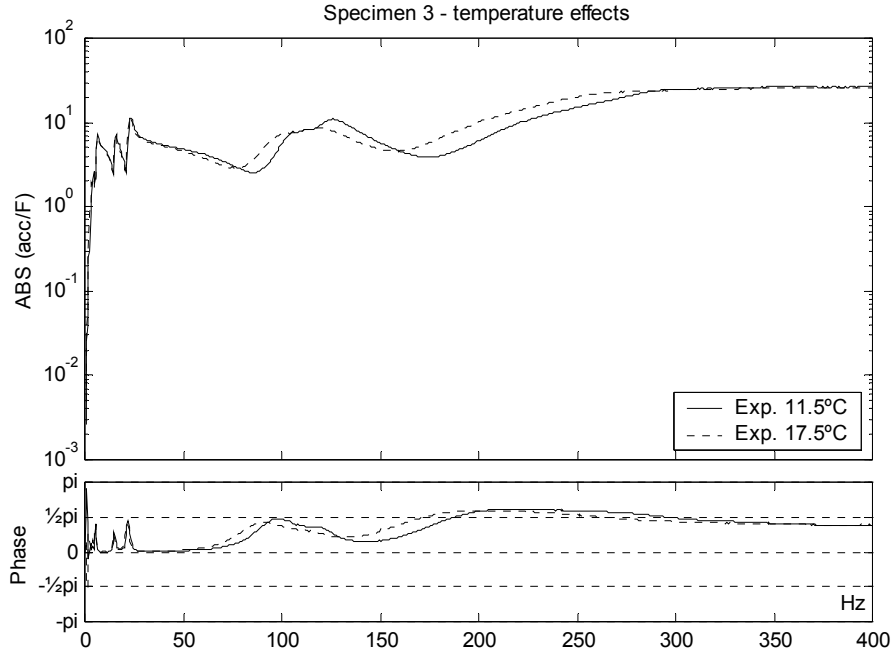


Fig.9: Frequency response functions of specimen 3 at temperatures 11.5°C and 17.5°C

3.2. CORRELATION OF NUMERICAL AND EXPERIMENTAL RESULTS

Overlaying the direct frequency response functions (magnitude and phase curves) measured on the four specimens with the numerically generated functions, it is possible to evaluate, by visual inspection, the overall level of correlation. It may be mentioned that for all specimens there are, as expected, a weak correlation in the low frequency range, due to the presence of the rigid body modes of the experimental set-up. Nevertheless, the first structural frequency is well above that frequency range.

In the next figures (Fig.10 to Fig.15) it is represented the comparison between the experimental and the numerical direct frequency response functions (accelerance). The numerical ones were generated by the finite element method using the model 2.

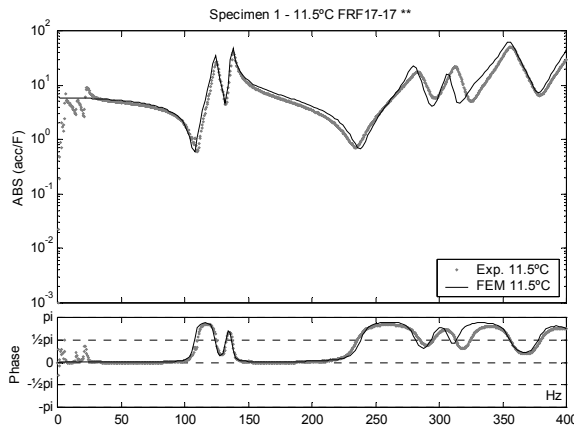


Fig.10: Frequency response functions of specimen 1 at temperature 11.5°C | experimental vs. numerical

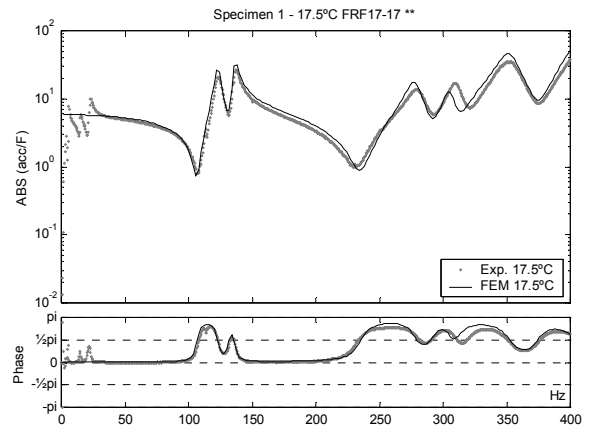


Fig.11: Frequency response functions of specimen 1 at temperature 17.5°C | experimental vs. numerical

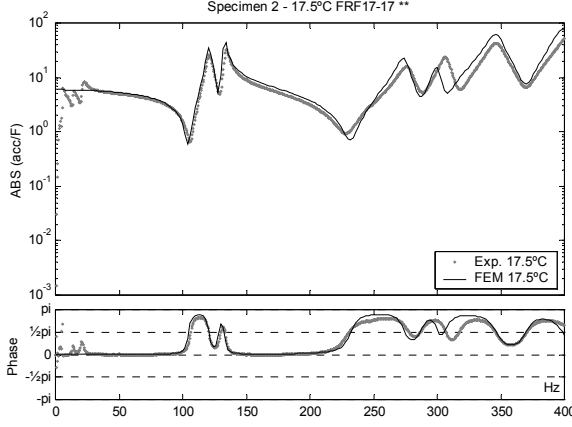


Fig.12: Frequency response functions of specimen 2 at temperature 17.5°C | experimental vs. numerical

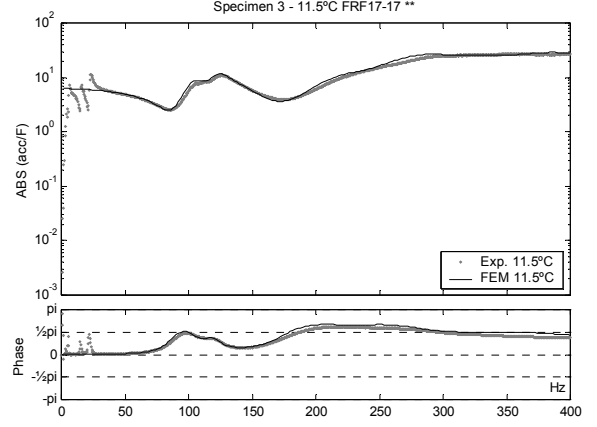


Fig.13: Frequency response functions of specimen 3 at temperature 11.5°C | experimental vs. numerical

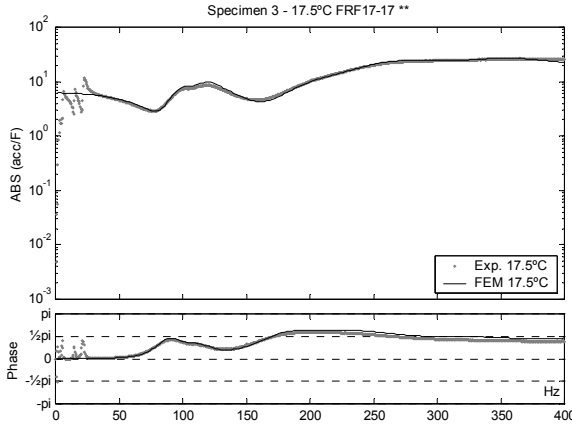


Fig.14: Frequency response functions of specimen 3 at temperature 17.5°C | experimental vs. numerical

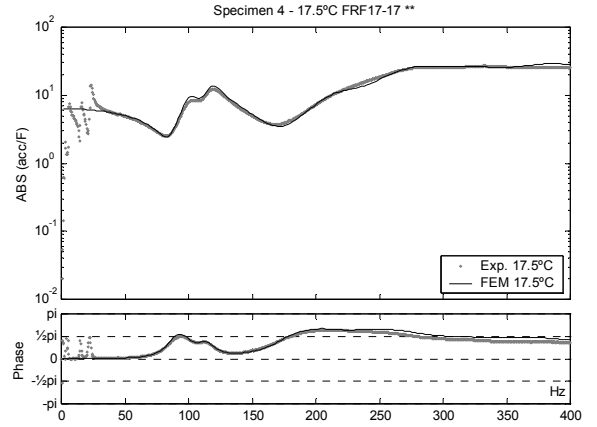


Fig.15: Frequency response functions of specimen 4 at temperature 17.5°C | experimental vs. numerical

The visual comparison of the overlaid curves provides a global idea of the correlation between the numerical results and the experimental data. The above represented functions, as well as the other functions of the response model, show a globally satisfactory overall correlation. However, such comparison does not quantify the level of the correlation and only provide a subjective and qualitative idea of it.

3.3 FRF-BASED CORRELATION INDICATORS

In order to obtain a quantitative measurement of the correlation between the numerical results obtained by the finite element model 2 and the experimental data, several frequency response functions correlation criteria available [12,13,14] were used.

The Frequency Response Assurance Criterion (*FRAC*) and the Frequency Amplitude Assurance Criterion (*FAAC*) provide a global correlation quality measurement for each degree of freedom over the whole frequency range.

$$FRAC_{jk} = \frac{|\{H_X(\omega_i)\}_{jk}^H \{H_A(\omega_i)\}_{jk}|^2}{(\{H_X(\omega_i)\}_{jk}^H \{H_X(\omega_i)\}_{jk})(\{H_A(\omega_i)\}_{jk}^H \{H_A(\omega_i)\}_{jk})} \quad (9)$$

$$FAAC_{jk} = \frac{2|\{H_X(\omega_i)\}_{jk}^H \{H_A(\omega_i)\}_{jk}|}{(\{H_X(\omega_i)\}_{jk}^H \{H_X(\omega_i)\}_{jk}) + (\{H_A(\omega_i)\}_{jk}^H \{H_A(\omega_i)\}_{jk})} \quad (10)$$

In the above expressions, $\{H_X(\omega_i)\}_{jk}$ and $\{H_A(\omega_i)\}_{jk}$ stand for, respectively, the experimental and numerical frequency response functions between the degrees of freedom j and k .

These indicators clearly outline the contribution of each degree of freedom on the overall response model correlation level. For specimens 1 and 3, tested and simulated at 17.5°C, these correlation indicators are represented in the Fig.16 and Fig.17, respectively.

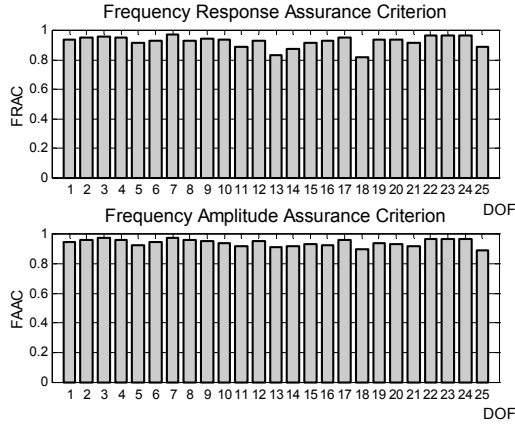


Fig.16: FRAC and FAAC correlation indicators for specimen 1 at temperature 17.5°C

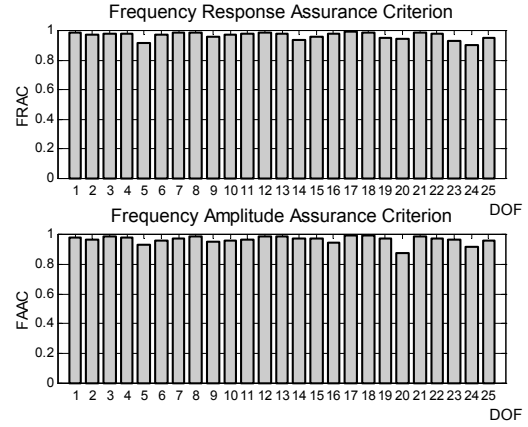


Fig.17: FRAC and FAAC correlation indicators for specimen 3 at temperature 17.5°C

On the other hand, the Global Shape Criterion (GSC) and the Global Amplitude Criterion (GAC) [14] quantify, as a function of frequency, the overall agreement, shape-based and amplitude-based, respectively, between the numerical results and the experimental data.

$$GSC(\omega) = \frac{|\{H_X(\omega)\}^H \{H_A(\omega)\}|^2}{(\{H_X(\omega)\}^H \{H_X(\omega)\})(\{H_A(\omega)\}^H \{H_A(\omega)\})} \quad (11)$$

$$GAC(\omega) = \frac{2|\{H_X(\omega)\}^H \{H_A(\omega)\}|}{(\{H_X(\omega)\}^H \{H_X(\omega)\}) + (\{H_A(\omega)\}^H \{H_A(\omega)\})} \quad (12)$$

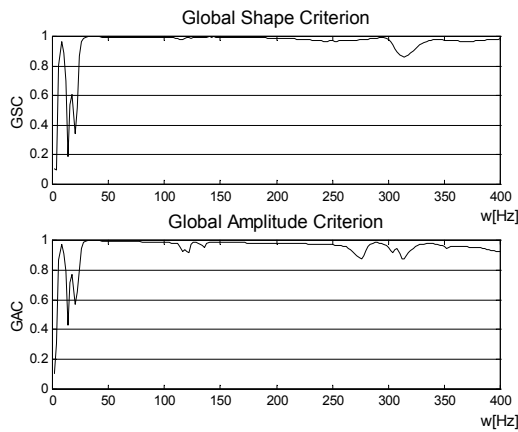


Fig.18: GSC and GAC correlation indicators for specimen 1 at temperature 17.5°C

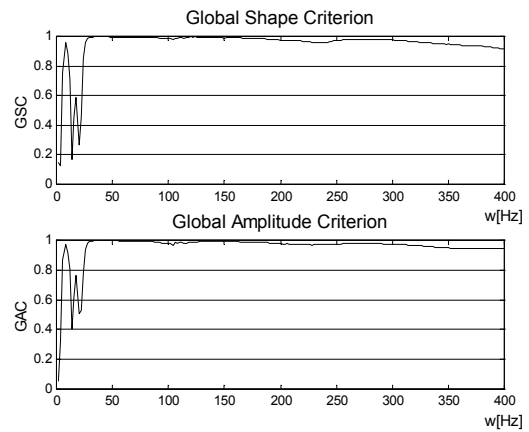


Fig.19: GSC and GAC correlation indicators for specimen 3 at temperature 17.5°C

The frequency distribution of these indicators for specimens 1 and 3 is represented in Fig.18 and Fig.19. For both criteria, global shape and global amplitude, a very satisfactory agreement is revealed between the experimental

and the numerical results within the bandwidth analysis. Moreover, with these criteria, the above mentioned rigid body modes effect in the low frequency range is well highlighted.

Another correlation criterion, the Local Amplitude Criterion (LAC) [14], is a helpful tool in the way that it quantifies the correlation between the numerical results and the experimental data as a frequency function for each individual degree of freedom. Thus, it is possible to individually evaluate the frequency correlation for each frequency response function.

$$LAC_{jk}(\omega) = \frac{2|(H_{Xjk}(\omega))^*(H_{Ajk}(\omega))|}{((H_{Xjk}(\omega))^*(H_{Ajk}(\omega))) + ((H_{Xjk}(\omega))^*(H_{Ajk}(\omega)))} \quad (13)$$

This indicator has been successfully applied in the identification of the error source verified on the previous global correlation indicators. From the results obtained, too extensive to be presented here, it was clearly identified which degrees of freedom and corresponding frequency ranges contribute to the decay of the overall correlation.

CONCLUSIONS

The passive damping treatments using viscoelastic material layers can provide an effective dynamic dissipative mechanism that can be applied with success in large and thin structures. The effectiveness of these treatments is closely related to the shear deformation energy dissipated by the viscoelastic layer.

This study has shown that the constrained and the integrated layer treatments can provide a simple, cost effective and reliable way to introduce the damping necessary for the dynamic control of resonant structures, even for low frequencies.

The dynamic behaviour of the treatments hereby studied can be effectively simulated using models based on the finite element method, thus making available an analysis tool that can be used in the design process to optimize the dynamic control of the treatments, as well as the structural behaviour of the application parts.

The three purposed models, based on a three-dimensional solid representation of the viscoelastic layer, were able to characterise the shear deformation pattern that occurs in it, leading to identical results.

Using the complex modulus approach in a frequency direct solving scheme it has been possible to easily introduce the frequency dependent viscoelastic properties into the numerical calculation procedure to generate the response model.

The validation of the finite element models was based on the correlation between the numerical and experimental frequency response functions of CLD and ILD plate specimens.

The application of frequency response functions based correlation indicators provided a correlation level evaluation that validates the finite element models used.

REFERENCES

1. Johnson, C.D., "Design of Passive Damping Systems", Special 50th Anniversary Design Issue, Transactions of the ASME, Vol.117, 1995, pp.171-176.
2. Nashif, A.D., Jones, D.I.G., Henderson, J.P., "Vibration Damping", John Wiley & Sons, 1985.
3. Jones, D.I.G., "Handbook of Viscoelastic Vibration Damping", John Wiley & Sons, 2001.
4. Moreira, R., Rodrigues, J., "Partial Viscoelastic Surface Damping Treatments", Book of Abstracts of Mechanics and Materials in Design 3, Orlando, USA, 2000, pp.171-172
5. Plouin, A., Balmès, E., "Steel/Viscoelastic/Steel Sandwich Shells Computational Methods and Experimental Validations", IMAC XVIII, 2000.
6. Plouin, A., Balmès, E., "A Test Validated Model of Plates with Constrained Viscoelastic Materials", IMAC XVII, 1999.
7. Taylor, D.W., "A Finite Element Modeling Approximation for Damping Material used in Constrained Damped Structures", Letters to the Editor, Journal of Sound and Vibration, Vol, 97-2, pp.352-354, 1984.
8. McTavish, D.J., Hughes, P.C., "Modeling of Linear Viscoelastic Space Structures", Journal of Vibration and Acoustics, Transactions of the ASME, Vol.115, 1993, pp.103-110.

9. Lesieutre, G.A., Mingori, D.L., "Finite Element Modelling of Frequency-Dependent Material Damping using Augmented Thermodynamic Fields", Journal of Guidance and Control, 1990.
10. Park, C.H., Inman, D.J., Lam, M.J., "Model Reduction of Viscoelastic Finite Element Models", Journal of Sound and Vibration, Vol. 219, Nr. 4, 1999, pp. 619-637.
11. 3M, "ScotchdampTM Vibration Control Systems, 3M Industrial Specialties Division, St. Paul, MN, 1993.
12. Ewins, D.J., "Modal Testing – Theory, Practice and Application", Second Edition, Research Studies Press, 2000.
13. Fotsch, D., Ewins, D.J., "Application of MAC in the Frequency Domain", IMAC XVIII, 2000.
14. Zang, C., Grafe, H., Imregun, M. "Frequency Criteria for Correlating and Updating Dynamic Finite Element Models", Mechanical Systems and Signal Processing, Vol 15-1, 2001, pp. 139-155.